THE JOURNAL OF BIOLOGICAL CHEMISTRY VOL. 283, NO. 33, pp. 22363–22370, August 15, 2008

BACH1 Is a Specific Repressor of *HMOX1* That Is Inactivated by Arsenite*[S]

Received for publication, March 5, 2008, and in revised form, June 10, 2008 Published, JBC Papers in Press, June 11, 2008, DOI 10.1074/jbc.M801784200

John F. Reichard[‡1], **Maureen A. Sartor**[§], **and Alvaro Puga**[§]

From the [§]*Department of Environmental Health and Center for Environmental Genetics, University of Cincinnati, Cincinnati, Ohio 45267 and the* [‡]*Department of Pediatrics, Division of Newborn Medicine, Children's Hospital Boston, Boston, Massachusetts 02115*

Intracellular heme is a redox active molecule that can be detrimental to cells at high concentrations or under oxidizing conditions. To prevent accumulation, the inducible enzyme heme oxygenase-1 (HMOX1) catalyzes degradation of heme. In the absence of elevated intracellular heme or oxidative stress, the basic region leucine zipper transcriptional regulator BACH1 binds HMOX1 antioxidant response elements and represses transcription. Conversely, increased intracellular heme or sulfhydryl oxidation inactivate BACH1, permitting transcriptional induction of HMOX1. Here, we investigate the effect of BACH1 inactivation on the induction of HMOX1 and as a mechanism for broader gene induction. We show that BACH1 is inactivated at low micromolar arsenite concentrations and that BACH1 inactivation is necessary and sufficient for transcriptional induction of HMOX1. Because BACH1 is thought to interact with antioxidant response element motifs, we further examined the role of BACH1 as a regulator of inducible antioxidant gene expression by assessing the global profile of gene expression following BACH1 knockdown using small interfering RNA. The loss of BACH1 function in human keratinocytes results almost exclusively in *HMOX1* induction, suggesting that BACH1 may function as a rheostat regulating levels of intracellular free heme.

Heme oxygenase (HMOX)[2] catalyzes the rate-limiting step of heme metabolism releasing carbon monoxide, iron, and biliverdin as products (1). Two heme oxygenase isoforms participate in heme metabolism: the inducible isoform heme oxygenase-1 (HMOX1) and the constitutive isoform heme oxygenase-2 (HMOX2). A third reported isoform, heme oxygenase-3, is considered to be a pseudogene processed from the HMOX2 transcript (2). HMOX1 induction is triggered by numerous forms of cellular stress, including transition metals (3, 4), heme and hemin (5–7), oxidants (8, 9), heat shock (10, 11), and hypoxia (12). In addition to metabolizing heme, HMOX1 reportedly protects against oxidative stress, a characteristic common to many HMOX1 inducers (13). The precise cytoprotective benefit of HMOX1 is unclear because HMOX1 itself does not directly catalyze an antioxidant reaction; however, removal of intracellular heme may be indirectly protective because (i) free intracellular heme is redox active; (ii) bilirubin, the product of biliverdin reduction, is an effective antioxidant; and (iii) iron released by heme degradation rapidly induces ferritin (14, 15).

Arsenite, the trivalent form of inorganic arsenic, is an environmental contaminant of major concern and a potent inducer of oxidative stress. Many of the effects of arsenite are attributable to its affinity for soft nucleophiles, particularly cysteine residues in glutathione and proteins (16). Arsenite rapidly oxidizes glutathione, thereby disrupting intracellular redox status (17), and forms covalent adducts with redox-sensitive protein sulfhydryls leading to protein dysfunction. In response to oxidative stress, such as that mediated by arsenite, cells induce a battery of protective antioxidant enzymes of which HMOX1 and thioredoxin reductase-1 (TXNRD1) are two well recognized members. This antioxidant response depends on stabilization and nuclear accumulation of the oxidant-activated transcription factor NFE2L2 (nuclear factor (erythroid-derived 2)-like 2, previously known as NRF2) (18–20), a basic region leucine zipper factor belonging to the MAF family of transcriptional regulators (21). To become transcriptionally active, nuclear NFE2L2 must heterodimerize with small MAF proteins and bind ARE enhancer motifs (22). The ARE is one form of MARE (MAF response element) having the core sequence RTGAYNNNGC (23–25). In addition to NFE2L2 binding, overlapping variants of this sequence can be recognized by other basic region leucine zipper factors (26). Such an arrangement appears to exist between NFE2L2 and BACH1 in the regulation of HMOX1 expression (24, 27) and between BACH1 and NF-E2 in the regulation of β-globin genes.

BACH1 (BTB and CNC homolog 1) is a MAF-related transcriptional repressor (28) that is conserved and ubiquitously expressed in tissues (29, 30). Although the global role of BACH1 as a regulator of gene expression is uncharacterized, BACH1 interacts with MARE-like enhancer sites recognized by NFE2L2 and NF-E2 (31, 32). BACH1 was originally characterized as a heme-regulated repressor of β-globin genes. Globin gene activation is regulated by the locus control region that contains several p45 NF-E2-binding elements. Through its

* This work was supported, in whole or in part, by National Institutes of Health Grants R01 ES10807 and P30 ES06096. The costs of publication of this article were defrayed in part by the payment of page charges. This article must therefore be hereby marked "*advertisement*" in accordance with 18 U.S.C. Section 1734 solely to indicate this fact.

[S] The on-line version of this article (available at http://www.jbc.org) contains supplemental data.

[1] Supported in part by NIEHS, National Institutes of Health Grant T32 ES07250 and an Environmental Carcinogenesis and Mutagenesis Training Grant. To whom correspondence should be addressed. Tel.: 617-919-4535; Fax: 617-730-0260; E-mail: john.reichard@childrens.harvard.edu.

[2] The abbreviations used are: HMOX, heme oxygenase; ARE, antioxidant response element; siRNA, small interfering RNA; ChIP, chromatin immunoprecipitation; PBS, phosphate-buffered saline; Q-PCR, quantitative real time PCR; PIPES, 1,4-piperazinediethanesulfonic acid; FDR, false discovery rate; TXNRD1, thioredoxin reductase-1; BACH1, BTB and CNC homolog 1; NFE2, nuclear factor erythroid-derived 2; NFE2L2, nuclear factor erythroid-derived 2-like 2; MAF, musculoaponeurotic fibrosarcoma.

interaction with these sites, BACH1 appears to recruit proteins that modify chromatin structure and regulate globin expression during erythroid differentiation (28, 29, 33). More recently BACH1 has been shown to antagonize NFE2L2-mediated induction of *HMOX1* through its interaction with multiple ARE/AP-1 sites (30, 34).

BACH1 may function as sensor of oxidative stress (7, 35, 36) that may mediate gene induction upon its inactivation. Structurally, human BACH1 contains 34 cysteine residues (37), at least six of which constitute cysteine/proline heme-binding domains that regulate DNA binding and nuclear export in response to elevated intracellular heme levels (35, 38). BACH1 binds MARE-like enhancer sequences in the absence of oxidative stress or elevated intracellular heme and appears to co-localize with repressive chromatin modifying factors that block gene transcription (32, 33). Increased heme or oxidative stress causes BACH1 to become inactivated, thereby permitting transcriptional activation by NF-E2 or NFE2L2.

Arsenite is a potent sulfhydryl-modifying agent capable of inactivating BACH1. Based on the observation that BACH1 interacts with NFE2L2 and NF-E2 enhancer elements, the present study investigates the global role of BACH1 inactivation as a mechanism for arsenite-mediated gene induction. We hypothesized that BACH1-mediated gene repression would be susceptible to low concentrations of arsenite and that inactivation of BACH1 would induce a subset of genes regulated by ARE- or NF-E2-like MARE motifs. Furthermore, the overlapping homology between the binding sequences recognized by MAF-related transcription factors (including MAF, NF-E2, Nrf1, Nrf2, and AP-1) (24, 32, 39) suggested the possibility that BACH1 inactivation could provide a mechanism by which environmentally relevant concentrations of arsenite, or other pro-oxidants, could induce an array of MARE-regulated genes.

We provide evidence that BACH1 inactivation causes NFE2L2-independent HMOX1 induction such as that mediated by hemin (the oxidized form of heme). Although BACH1 inactivation is an effective mediator of HMOX1 induction, we show that this is not a generalized mechanism controlling expression of MARE-regulated genes. Rather, chromatin immunoprecipitation (ChIP) experiments and expression miroarrray data show that BACH1 plays a specific role in sensing and regulating HMOX-dependent heme turnover. Thus, BACH1 maintains intracellular heme homeostasis by functioning as a fulcrum that balances intracellular heme levels with cellular redox status through the expression of HMOX1.

MATERIALS AND METHODS

Cells and Chemical Treatments—HaCaT human keratinocytes (40) were grown in Dulbecco's modified Eagle's medium (Mediatech, Herndon, VA) supplemented with 5% fetal bovine serum (Sigma-Aldrich) and 1% penicillin-streptomycin solution (Invitrogen). The cells were incubated at 37 °C with 5% CO_2 and grown to ~90% confluence before treatment. Aqueous solutions of $NaAsO_2$ (hereafter referred to as arsenite) (Sigma-Aldrich) were prepared from a 1000× stock in double distilled H_2O.

Whole Cell Extracts, Nuclear Extracts, and Immunoblotting—For preparation of whole cell extracts, the cells were washed and harvested in PBS containing 1× Complete protease inhibitor mixture (Roche Applied Science) and lysed by sonication (Sonic Dismembrator 60; Fisher) on ice three times for 10 s in 300 μl of NETN buffer (100 mM NaCl, 20 mM Tris, pH 8.0, 1 mM EDTA, 0.5% Nonidet P-40; Complete protease inhibitor). Nuclear extracts were prepared using a nuclear extraction kit from Panomics (Fremont, CA) according to the manufacturer's protocol. Protein concentrations were measured using the Bradford assay and concentrations adjusted to 1 μg/μl. Total cellular proteins (20 μg) or nuclear lysates (10 μg) were separated by SDS-PAGE, transferred to polyvinylidene difluoride, and probed for NFE2L2 (H300; Santa Cruz Biotechnology), β-actin (Sigma), HMOX1 (C20; Santa Cruz Biotechnology), in blocking buffer containing 3% nonfat dry milk in PBST (0.1 M PBS with 0.2% Tween 20). The blots were probed for BACH1 (C20; Santa Cruz Biotechnology) in blocking buffer containing 1% bovine serum albumin in PBST. After washing, the blots were incubated with species-appropriate horseradish peroxidase-conjugated secondary antibody (Santa Cruz), incubated with chemiluminescent reagent (PicoWest Super Signal; Pierce) and visualized by exposing to film (GE Healthcare).

RNA Isolation and Real Time Reverse Transcription-PCR—Total RNA was extracted using NucleoSpin RNA II columns (Macherey-Nage, Bethlehem, PA) according to manufacturer instructions. cDNA was synthesized by reverse transcription of 1 μg of total RNA in a total volume of 20 μl containing 1× reverse transcriptase buffer (Invitrogen), 25 μg/ml oligo$(dT)_{12-18}$ (Invitrogen), 0.5 mM dNTP mix (GeneChoice, Frederick, MD), 10 mM dithiothreitol (Invitrogen), 20 units of RNase inhibitor (RNasin®; Promega, Madison WI), and 100 units of SuperScript™ II reverse transcriptase (Invitrogen). The resulting cDNA products were diluted in a final volume of 200 μl, and a 2-μl aliquot was used as template for subsequent quantification by real time PCR (Q-PCR) amplification. Q-PCR was performed in a 25-μl reaction mixture containing 1× Clontech QTaq polymerase reaction mix (Mountain View, CA), 1× SybrGreen (Invitrogen) as a marker of amplification, 0.1 μM of each primer, and 2 μl of template cDNA. The products were amplified with human HMOX1 primers (forward, 5′-CTCAAACCTCCAAAAGCC-3′ and reverse, 5′-TCAAAAACCACCCCAACCC-3′), TXNRD1 primers (forward, 5′-CTTTTTCATTCCTGCTA CTCTACC-3′ and reverse, 5′-CTCTCTCCTTTTCCCTTTTCC-3′), BACH1 primers (forward, 5′-TGCGATGTCACCATCTTTGT-3′ and reverse, 5′-CCTGGCCTACGATTCTTGAG-3′), and glyceraldehyde-3-phosphate dehydrogenase primers (forward, 5′-GATC-ATCAGCAATGCCTCCT and reverse, TGTGGTCATGAGTC-CTTCCA. Amplifications were performed using an Opticon 2 Q-PCR detection system (MJ Research). The cycle threshold (C_t) of each sample was automatically determined to be the first cycle at which a significant increase in optical signal above an arbitrary base line was detected. Amplification of β-actin cDNA in the same samples was used as an internal control for all PCR amplification reactions. Relative mRNA expression was quantified using the comparative C_t (ΔC_t) method and expressed as $2^{-(\Delta\Delta C_t)}$. Each PCR assay was done in triplicate.

ChIP Analysis—The nuclei were isolated from formaldehyde (1% final) fixed cells by lysing cells in buffer containing 5 mM PIPES, pH 8.0, 85 mM KCl, 0.5% Nonidet P-40, and 1× Com-

plete protease inhibitor. DNA was fragmented by sonication using a Diagenode Bioruptor in nuclear lysis buffer containing 50 mM Tris-HCl, pH 8.1, 10 mM EDTA, 1% SDS, and 1× Complete protease inhibitor. DNA-cross-linked proteins were either immunoprecipitated from precleared samples using 2–5 μg of antibody, including anti-NFE2L2, anti-BACH1 or rabbit IgG control (Millipore), or used as total input chromatin. The antibodies were pulled down with protein A beads at 4 °C overnight. Recovered beads were resuspended in 1× dialysis buffer (2 mM EDTA, 50 mM Tris-HCl, pH 8.0, 0.2% Sarkosyl, and 1× Complete protease inhibitor) and washed twice with dialysis buffer, followed by four washes with immunoprecipitation wash buffer (100 mM Tris-HCl, pH 9.0, 500 mM LiCl, 1% Nonidet P-40, 1% deoxycholic acid, and 1× Complete protease inhibitor). Antibody-chromatin complexes were eluted in immunoprecipitation elution buffer (50 mM $NaHCO_3$, 1% SDS) with vigorous shaking. Immunoprecipitated DNA and total input chromatin were diluted with water and brought up to 0.3 M NaCl, and cross-linking was reversed at 65 °C overnight following the addition of RNase A. The following morning, samples were digested with proteinase K at 45 °C for 2 h. DNA was purified using the Qiaquick PCR purification kit (Qiagen) as per the manufacturer's protocols. The samples were evaluated for enrichment by Q-PCR in a 25-μl reaction mixture containing 1× BD QTaq polymerase reaction mix (BD Biosciences), 1× SybrGreen (Invitrogen) as a marker of DNA amplification, and 0.1 μM of each primer. Relative enrichment was determined using Q-PCR primers for *HMOX1* EN2 (forward, 5′-CACGGTCCCGAGGTCTATT and reverse, 5′-TAGACCGTGACTCAGCGAAA), *HMOX1* EN1 (forward, 5′-CAGTGCCTCCTCAGCTTCTC and reverse, 5′-CTCGGTGGATTGCAACATTA), and TXNRD1 (forward, 5′-ACGAGGAGTGGATTTCTGCTT and reverse, 5′-AGGGTTGCTGTTTCCTAATGG). The relative efficiency of each PCR primer was determined using input DNA and adjusted accordingly. The DNA in each immunoprecipitated sample was normalized to the corresponding input chromatin (ΔC_t), and enrichment was defined as the change in C_t in treated samples relative to untreated controls ($\Delta\Delta C_t$) and IgG negative controls. Exponential $\Delta\Delta C_t$ values were converted to linear values ($2^{-(\Delta\Delta C_t)}$) for graphical presentation as either fold change or percent change, where indicated.

Microarray Hybridization—Control samples were co-hybridized with the two BACH1 knockdown samples in triplicate, with one dye-flip for each comparison. For each condition, three independent samples were generated for microarray analyses. Total RNA was isolated as described above for microarray analysis from each independent biological replicate ($n = 3$ per condition). Microarray experiments were carried out essentially as previously described (41, 42) with minor modifications. The Operon Array-Ready mouse genome oligonucleotide set consisting of 31,769 optimized 70-mer oligonucleotides was used to make microarrays (Qiagen). The oligonucleotides were suspended in 3× SSC at 30 μM and printed at 22 °C and 65% relative humidity on aminosilane-coated slides (Cel Associates, Inc., Pearland, TX) using a high speed robotic Omnigrid machine (GeneMachines, San Carlos, CA) with Stealth SMP3 pins (Telechem, Sunnyvale, CA). Fluorescence-labeled cDNAs were synthesized from total RNA using an indirect amino allyl labeling method via an oligo(dT)-primed, reverse transcriptase reaction. The hybridizations were performed using the MAUI hybridization system at 48 °C (BioMicro Systems, Inc, Salt Lake City, UT). The imaging and data generation were carried out using a GenePix 4000A and GenePix 4000B (Axon Instruments, Union City, CA) and associated software from Axon Instruments, Inc. The microarray slides were scanned with dual lasers with wavelength frequencies to excite Cy3 and Cy5 fluorescence emission. The images were captured in JPEG and TIFF files, and the DNA spots were captured by the adaptive circle segmentation method. The Cy3 and Cy5 fluorescence signal intensities were normalized.

Statistical Analysis of Microarrays—The data representing generated by GenePix® Pro version 5.0 software were analyzed to identify differentially expressed genes (43). Data normalization was performed in two steps for each microarray separately (41, 42). First, background adjusted intensities were log-transformed and the differences (M) and averages (A) of log-transformed values were calculated as $M = \log_2(X1) - \log_2(X2)$ and $A = [\log_2(X1) + \log_2(X2)]/2$, where X1 and X2 denote the Cy5 and Cy3 intensities, respectively. Second, normalization was performed by fitting the array-specific local regression model of M as a function of A. Normalized log intensities for the two channels were then calculated by adding half of the normalized ratio to A for the Cy5 channel and subtracting half of the normalized ratio from A for the Cy3 channel. Statistical analysis was performed for each gene separately by fitting an analysis of variance model (44). The resulting t statistics comparing each BACH1 knockdown *versus* control were modified using IBMT, an intensity-based empirical Bayesian moderated t statistic (45). Estimates of fold change were calculated, and genes with p value <0.01, fold change > 1.5, and average spot intensity > 100 in both siRNAs, or false discovery rate (FDR) < 0.10 in either single siRNA, were considered for follow-up. Data analysis was performed using the statistical software R and the Bioconductor platform.

RESULTS

HMOX1 and TXNRD1 Are Induced Differently by Arsenite—Arsenite is a potent thiol oxidant and a well characterized inducer of a host of genes, including several that transcribe enzymes protective against oxidative stress (17). Because skin is an important site of arsenic toxicity, the concentration-dependent antioxidant response to arsenite was investigated in human keratinocyte-derived HaCaT cells. Both HMOX1 and TXNRD1 are highly inducible by arsenite, at least in part through the activation of NFE2L2; however, HMOX1 expression is also influenced by BACH1, whereas TXNRD1 is not (7). As shown in Fig. 1, 6 h of continuous exposure to arsenite induces expression of both genes; however, the concentration responses of induction differs markedly between these two genes, particularly at very low arsenite concentrations (≤1.0 μM) where TXNRD1 is measurably induced, whereas HMOX1 is not. With increasing arsenite concentrations, the response of TXNRD1 is essentially linear (Fig. 1, *inset*), whereas HMOX1 is induced only at concentrations greater than 1 μM. These concentration response curves suggest that BACH1 may inhibit HMOX1 induction at low arsenite concentrations.

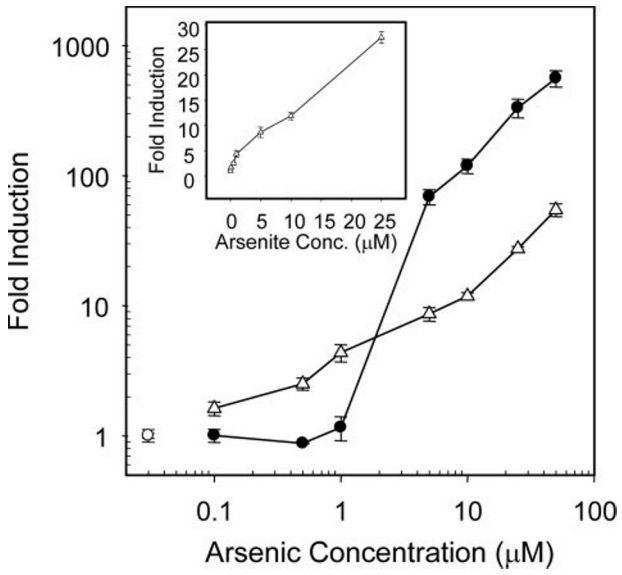

FIGURE 1. **Concentration-dependent induction of HMOX1 and TXNRD1 by arsenite.** HMOX1 (*circles*) and TXNRD1 (*triangles*) mRNA expression levels in HaCaT cells continuously treated for 6 h with the indicated concentration (*Conc.*) of arsenite. Cellular mRNA levels were determined by Q-PCR. The concentrations were normalized to β-actin mRNA levels for each sample and expressed as fold change relative to untreated controls. *Inset*, linear presentation of TXNRD1 mRNA levels following treatment with the indicated concentration of arsenite. The values represent at least three independent experiments quantified in triplicate.

Activation of NFE2L2 and Inactivation of BACH1 Transcription Factors by Arsenite—The concentration-dependent activation of NFE2L2 and inactivation of BACH1 were investigated by examining the presence of these two transcription factors in nuclear extracts 3 h after arsenite treatment. In Fig. 2, immunoblots of nuclear and cytosolic extracts showed a marked decrease in nuclear levels of BACH1 with concentrations of arsenite as low as 0.1 μM, whereas the lowest concentration of arsenite to elicit nuclear accumulation of NFE2L2 was 5 μM, with significantly greater accumulation at 25 μM treatment. These data suggest that submicromolar arsenite concentrations are capable of inactivate BACH1. In comparison, the minimum concentration of arsenite necessary to achieve NFE2L2 activation, as indicated by protein nuclear localization, is in the range of 5 μM.

A more physiologically meaningful indicator of transcription factor activation is its binding to DNA. ChIP assays were utilized to evaluate DNA binding of these factors at HMOX1 enhancer elements. Two enhancer regions of HMOX1 were evaluated for NFE2L2 and BACH1 binding before and after arsenite treatment: a proximal element consisting of two motifs starting at 3928 bp from the transcription start site (EN1) and a distal element consisting of 4 identical repeat elements starting 9076 bp from the transcription start site (EN2) (Fig. 3*A*). In cells naïve to arsenite, little NFE2L2 is bound to either site, whereas BACH1 is highly bound to both elements (Fig. 3*B*). Conversely, following treatment with 25 μM arsenite, NFE2L2 is highly bound at both elements, and BACH1 binding is lost. Evaluation of NFE2L2 and BACH1 binding throughout the remaining regions shows no additional binding sites (7).

To determine whether BACH1 and NFE2L2 respond differently to arsenite, particularly at low concentrations, DNA binding of BACH1 and NFE2L2 was evaluated over a range of arsenite concentrations. As expected, BACH1 binding at the EN1 (Fig. 4*A*) and EN2 (Fig. 4*B*) enhancer elements is progressively lost with increasing arsenite concentrations. At the lowest concentrations affecting DNA binding (0.5 and 1 μM), there is a fractional loss of BACH1, with weak binding by both NFE2L2 (Fig. 4, *C* and *D*) and RNA polymerase II (Fig. 4*E*). At 1 μM arsenite, BACH1 is still greater than 50% bound to both enhancer elements. As arsenite concentrations exceed 5 μM, the loss of BACH1 binding is nearly complete; however, BACH1 removal is also accompanied by increased NFE2L2 DNA binding at both enhancer sites (Fig. 4, *C* and *D*) consistent with the observed NFE2L2 nuclear accumulation (Fig. 2). Reciprocal loss of DNA-bound BACH1 and increased NFE2L2

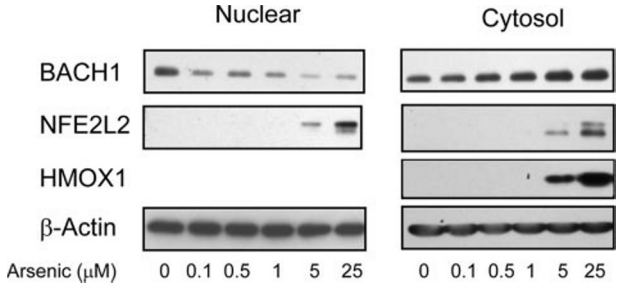

FIGURE 2. **NFE2L2 and BACH1 are reciprocally activated by arsenite.** Immunoblots of nuclear (*left panels*) or cytosolic (*right panels*) lysates show changes in subcellular localization of NFE2L2 and BACH1 associated with the indicated arsenite treatments. The cells were continuously treated with arsenite for 3 h prior to lysis. β-Actin serves as an internal loading control. The blots are representative of two or three separate experiments.

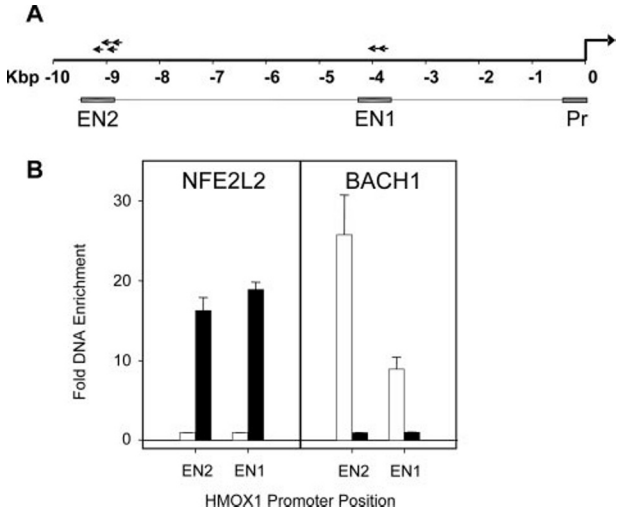

FIGURE 3. **NFE2L2 and BACH1 reciprocally interact with distal enhancer sites of *HMOX1*.** *A*, the positions of the EN1 and EN2 enhancer motifs, relative to the *HMOX1* transcription start site as annotated by the NCBI Homo *sapiens* Genome Map Viewer, Build 36.2. *Arrows* indicate the plus-strand orientation of each ARE motif in that region relative to the consensus ARE sequence (5′-RTGAYnnnGC). *B*, NFE2L2 (*left panel*) and BACH1 (*right panel*) binding at the EN1 (−3928 bp) and EN2 (−8979 bp) sites as determined by quantitative ChIP assays. Immunoprecipitated DNA from untreated control cells (*open bars*) or cells treated for 3 h with 25 μM arsenite (*filled bars*) was analyzed for enrichment by Q-PCR using primers amplifying DNA in the vicinity of the ARE motifs. Amplification is expressed as fold enrichment by normalizing the C_t for each primer in chromatin immunoprecipitated samples to the C_t obtained from the respective input DNA and expressing these values relative to samples containing the DNA-unbound transcription factor (control samples for NFE2L2 and arsenite treated for BACH1). The values represent the means ± S.E. of at three independent experiments performed in triplicate.

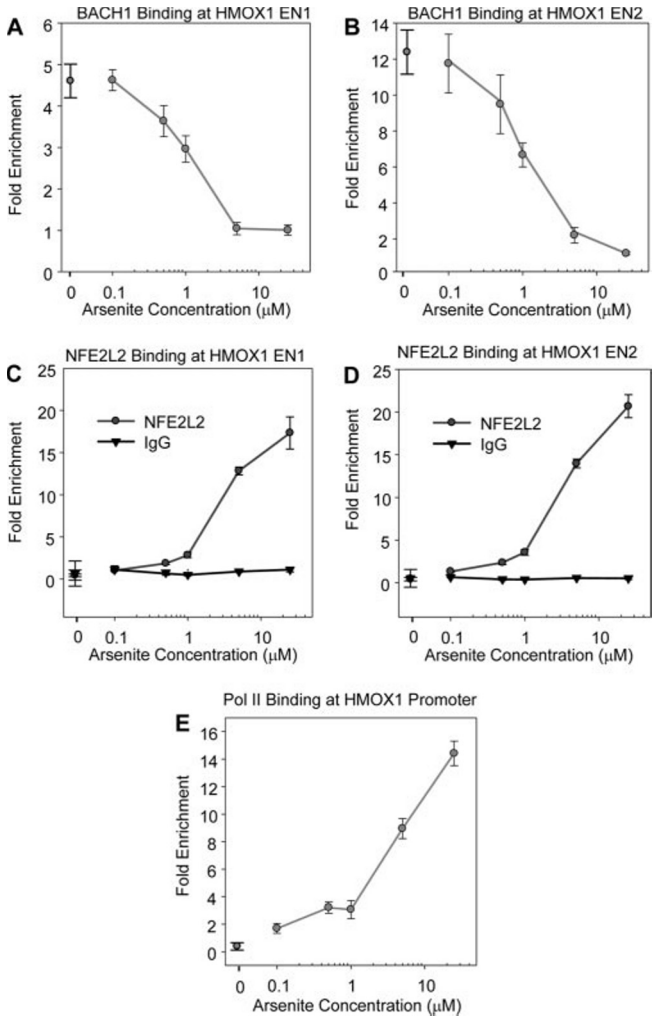

FIGURE 4. **NFE2L2 and BACH1 reciprocally bind DNA and are associated with transcriptional activation of *HMOX1*.** Time course of DNA binding by BACH1 (*A* and *B*), NFE2L2 (*C* and *D*), and DNA polymerase II (*E*) following treatment with the indicated concentration of arsenite. ChIP-enriched DNA was quantified using Q-PCR with primers flanking the *HMOX1* ARE motifs at positions −3992 (*A* and *C*) −8979 (*B* and *D*) and −148 (RNA polymerase II). Fold binding is the value for each treatment normalized to its corresponding input and expressed relative to the value associated with the DNA-unbound factor (control samples for NFE2L2 and arsenite treated for BACH1). The figure shows the results of two independent experiments performed in triplicate ± S.E.

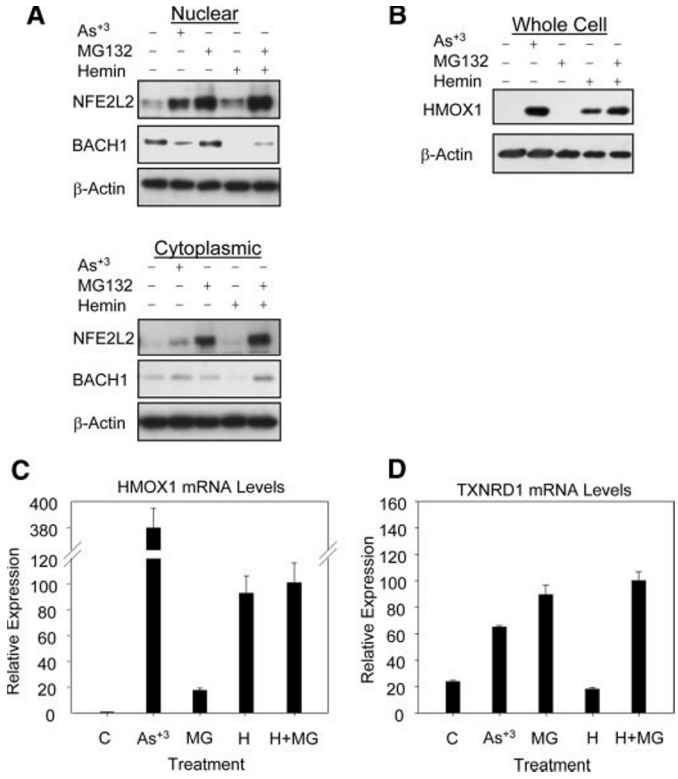

FIGURE 5. **HMOX1 and *TXNRD1* can be differentially regulated by dissociating BACH1 and NFE2L2 activation.** *A*, immunoblots of proteins from nuclear (10 μg/lane) and cytoplasmic (20 μg/lane) lysates illustrating differential localization of NFE2L2 and BACH1 protein following 3 h of treatment of HaCaT cells with 25 μM arsenite, 5 μM MG132, 25 μM hemin, or combined treatment with MG132 + hemin. *B*, immunoblots of proteins from whole cell lysates (20 μg/lane) 6 h after treatment as in *A*. The blots are representative of two or three separate experiments. Messenger RNA levels of HMOX1 (*C*) and TXNRD1 (*D*) quantitated following treatment with 25 μM arsenite, 5 μM MG132, 25 μM hemin, or combined treatment with MG132 + hemin. Relative mRNA levels were determined by Q-PCR, normalized to β-actin levels and expressed as percentages of the expression associated with Heme+MG132 treatment. The values represent at least three independent experiments quantified in triplicate ± S.E.

binding also corresponds with markedly increased RNA polymerase II binding at the HMOX1 promoter, indicating transcriptional activation at these low micromolar concentrations. Taken together, these data show that BACH1 DNA binding is more sensitive to low dose arsenite exposure than is NFE2L2; however, concentrations that do not trigger nuclear NFE2L2 accumulation only partially inactivate BACH1. This is in comparison with higher arsenite concentrations that extensively inactivate BACH1 while also stimulating a pronounced increase in NFE2L2 activation. Therefore, to further investigate BACH1 inactivation as a mechanism of gene induction, it was necessary to dissociate BACH1 inactivation from NFE2L2 activation.

Inactivation of BACH1 Is Sufficient to Induce HMOX1—Hemin is known to induce HMOX1 through inactivation of BACH1. Contrastingly, the proteasome inhibitor MG132 induces ARE-regulated genes, including HMOX1, through stabilization of *de novo* synthesized NFE2L2. To test the relative roles of BACH1 and NFE2L2 in the induction of HMOX1, HaCaT cells were treated with MG132 or hemin to differentially regulate the activity of NFE2L2 and BACH1, respectively. Proteasome inhibition by MG132 causes nuclear accumulation of NFE2L2 with little effect on nuclear BACH1 levels (Fig. 5*A*). In comparison, hemin treatment triggers loss of BACH1 from the nucleus without triggering NFE2L2 accumulation. As expected, arsenite causes simultaneous accumulation of nuclear NFE2L2 and export of nuclear BACH1 in a manner comparable with combined treatment with hemin and MG132. Thus, inactivation of BACH1 is associated with pronounced HMOX1 protein induction, whereas MG132 does not mediate HMOX1 induction despite the accumulation of high levels of nuclear NFE2L2 (Fig. 5*B*).

Although both HMOX1 and TXNRD1 are regulated through ARE enhancer elements, BACH1 does not interact with the *TXNRD1* enhancer (7). Thus, we find that hemin treatment strongly induces HMOX1 and has no effect on TXNRD1 (Fig. 5*C*). In comparison, MG132 is a relatively weak inducer of HMOX1 but strongly induces TXNRD1 (Fig. 5*D*). This shows

that, in the absence of BACH1 involvement, NFE2L2 readily mediates gene induction; however, the presence of BACH1 significantly inhibits transcriptional induction mediated by NFE2L2. It may be important to note that arsenite induces HMOX1 mRNA and protein expression to a much greater extent than either hemin alone or combined treatment with hemin and MG132, suggesting involvement of additional transcriptional activators, possibly including heat shock factor(s). This contrasts with TXNRD1 where induction by arsenite does not exceed that caused by MG132 alone.

To examine the extent to which BACH1 is specifically responsible for repressing gene expression, BACH1 was knocked down by transiently transfecting cells with siRNA constructs targeting two different regions of the BACH1 transcript. The effect of each BACH1-specific siRNA was measured relative to a nonsense negative control siRNA and siRNA specific for glyceraldehyde-3-phosphate dehydrogenase. Forty-eight hours after transfection, both BACH1-specific siRNAs reduce BACH1 protein to nearly undetectable levels, whereas negative control siRNA has no effect on BACH1 (Fig. 6*A*). Similarly, both BACH1-specific siRNAs significantly reduce BACH1 mRNA transcript levels relative to cells transfected with negative control siRNAs (Fig. 6*B*). Thus, BACH1-specific knockdown, in the absence of any additional treatment, causes significant HMOX1 induction (Fig. 6*C*), thereby showing that the loss of BACH1 repression is sufficient to trigger HMOX1 induction in the absence of any additional treatment.

BACH1 Is a Specific Repressor of HMOX1 Gene Expression—Through its interactions with MARE-like enhancers, it is possible that BACH1 inactivation by heme and pro-oxidants might induce a broad array of genes. Thus, it is of interest to identify genes, in addition to HMOX1, that are coordinately regulated through BACH1 inactivation. To globally investigate genes induced or repressed by the loss of BACH1 repression, we analyzed HaCaT cells for changes in gene expression by microarray analysis following BACH1 knockdown. Using two different BACH1 siRNAs, the cells were separately transfected with each siRNA 48 h prior to mRNA analysis. Transfections were performed in triplicate and comparisons made relative to control cells transfected in parallel with a nonsense siRNA. Changes in gene expression were considered important when the p value was <0.01 and the fold change in expression relative to negative controls was 1.5-fold or greater for both siRNAs or where an FDR was <0.10 in either siRNA. Table 1 summarizes up-regulated genes in two sections: genes that are up-regulated by both siRNAs and genes that are up-regulated only by siRNA 1 or siRNA 2. For each gene, the level of expression and p value are presented. We find that only a handful of genes are commonly induced by both BACH1 siRNAs. With the notable exception of HMOX1, none of the genes significantly induced by loss of BACH1 increase greater than 1.5–3-fold control levels, nor do any have well characterized biologic functions. Conversely, the loss of BACH1 does not appear to down-regulate gene expression because no single gene is consistently down-regulated by the two anti-BACH1 siRNAs (supplemental data). Among genes that are affected by loss of BACH1, HMOX1 has by far the lowest FDR (<0.0001) and is the only gene with an FDR < 0.1 for both siRNA constructs. These data further corroborate

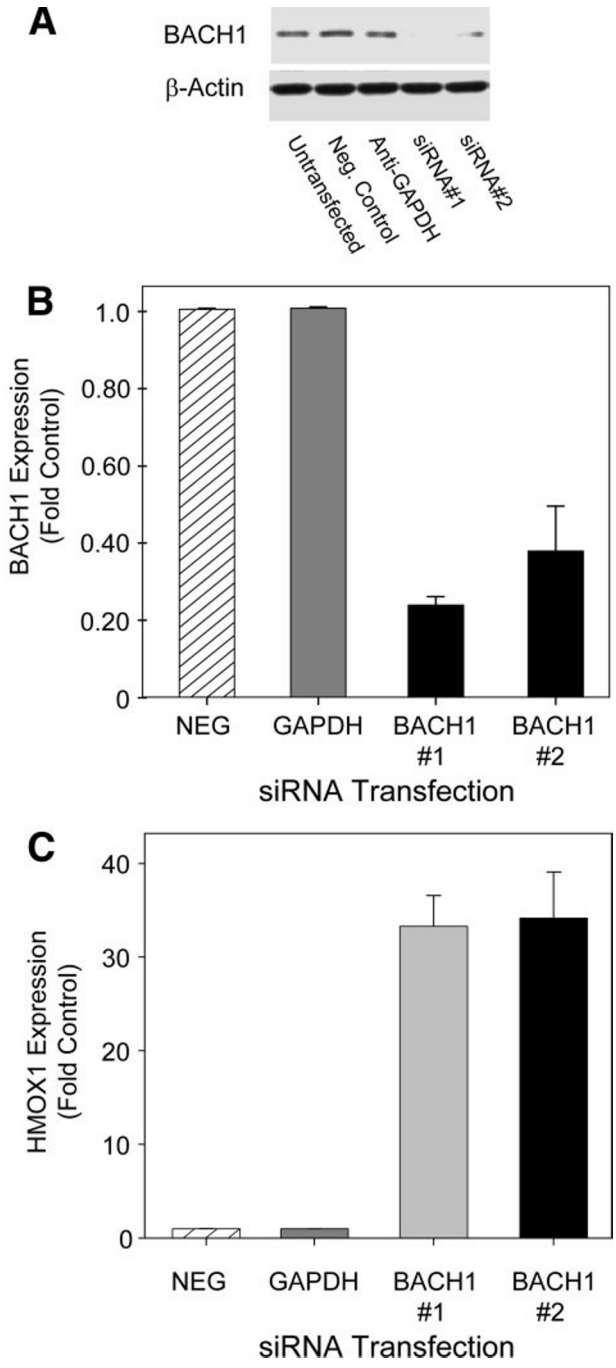

FIGURE 6. **Knockdown of BACH1 by siRNA induces HMOX1 expression independent of NFE2L2 activation.** *A*, representative immunoblot of whole cell lysates (20 μg/lane) probed with antibody against BACH1 48 h after transfection with nonspecific negative (*NEG*) control siRNA, siRNA specific for glyceraldehyde-3-phosphate dehydrogenase or siRNA specific for BACH1. *B*, relative levels of BACH1 mRNA 48 h after transfection with the indicated siRNA. *C*, relative expression levels of HMOX1 mRNA 48 h after transfection with the indicated siRNA. Relative mRNA levels were determined by Q-PCR, normalized to β-actin mRNA levels, and expressed as fold expression relative to cells transfected with negative control siRNA. The values represent at least three independent experiments quantified in triplicate ± S.E.

Q-PCR data that shows inactivation or loss of BACH1-mediated repression permits high level HMOX1 transcription. More importantly, HMOX1 is the one and only gene to show >2-fold change for both siRNA knockdowns when BACH1 repression is lost.

TABLE 1

Gene induction following knockdown of BACH1 using two siRNA constructs targeting different regions of the BACH1 transcript

Genes that were significantly ($p < 0.01$) induced by both siRNA constructs are presented in the top section, whereas genes significantly ($p < 0.001$) induced by one siRNA but not the other are presented in the lower section. The genes are ranked in order of expression levels presented in either column 5 (siRNA 1) or column 7 (siRNA 2). Fold change and p values for both BACH1 siRNAs are presented. The gene expression levels were determined 48 h after BACH1 knockdown and expressed relative to cells transfected with negative control siRNA. Genes that appear multiple times for single siRNA had multiple probes on the array that met the criteria for statistical significance.

	GenBank™ accession number	Name	Symbol	LocusID	BACH1 siRNA 1		BACH1 siRNA 2	
					Fold change	p value	Fold change	p value
Genes induced by both siRNA 1 and siRNA 2	NM_002133	Heme oxygenase (decycling) 1	HMOX1	3162	26.66	4.56E-10	12.50	4.45E-09
	NM_002133	Heme oxygenase (decycling) 1	HMOX1	3162	19.88	1.19E-10	14.34	1.08E-09
	NM_006515	SET domain and mariner transposase fusion gene	SETMAR	6419	3.59	1.81E-05	1.70	7.57E-03
	BC010608	REST corepressor 2	RCOR2	283248	2.09	2.32E-03	1.53	1.37E-03
	AL354613	Transmembrane protein 48	TMEM48	55706	1.80	1.74E-03	1.97	7.12E-04
	NM_006012	ClpP caseinolytic peptidase, ATP-dependent, proteolytic homolog	CLPP	8192	1.69	1.48E-03	1.54	6.46E-04
	NM_003405	Tyr 3-monooxygenase/Trp 5-monooxygenase activation protein	YWHAH	7533	1.63	2.12E-03	1.71	1.09E-03
	NM_018234	STEAP family member 3	STEAP3	55240	1.52	6.64E-03	1.50	7.99E-03
	NM_024536	Chondroitin polymerizing factor	CHPF	79586	1.52	1.13E-04	1.73	1.41E-05
	NM_002184	Interleukin 6 signal transducer (gp130, oncostatin M receptor)	IL6ST	3572	1.52	8.23E-03	1.58	4.96E-03
Genes induced by either BACH1 siRNA 1 or siRNA 2	AK057614	Immunoglobulin heavy constant mu	IGHM	3507	4.05	5.09E-04	−1.11	3.90E-01
	NM_006082	α-Tubulin	K-α-1	10376	−1.14	1.50E-01	3.78	6.43E-05
	NM_032271	Tumor necrosis factor receptor-associated factor 7	TRAF7	84231	1.31	2.71E-02	2.03	3.43E-04
	NM_033657	Death-associated protein 3	DAP3	7818	1.47	2.02E-02	1.87	3.74E-05
	AK056821	SAR1 gene homolog B	SAR1B	51128	1.40	7.44E-04	1.65	1.76E-04
	AL049265	Interleukin 6 signal transducer	IL6ST	3572	1.10	2.66E-01	1.65	1.98E-04
	NM_031943	Eukaryotic translation initiation factor 3, subunit 5	IFP38	83880	1.36	9.95E-03	1.58	9.03E-04
	Y10183	Activated leukocyte cell adhesion molecule	ALCAM	214	1.40	1.66E-04	1.50	3.78E-05

DISCUSSION

Although transcriptional activation of ARE-regulated genes by the redox sensitive KEAP1/NFE2L2 pathway has been well characterized, the importance of the transcriptional repressor BACH1 has not. Here, the possibility that BACH1 may act globally as a redox-sensitive repressor of genes under control of ARE or NF-E2 enhancer elements was investigated. However, as our present data indicate, BACH1 inactivation is not associated with broad induction of either ARE or NF-E2 regulated genes; rather, BACH1 appears to be the primary regulator of intracellular heme metabolism through specific induction of HMOX1.

Using keratinocyte-derived HaCaT cells we investigated the role of BACH1 as a potential target for oxidative gene expression regulation. It was initially observed that although HMOX1 is induced to very high levels by arsenite, HMOX1 remains repressed at arsenite concentrations that effectively induce other ARE-regulated genes, such as *TXNRD1*, NAD(P)H dehydrogenase, quinone 1 (*NQO1*), glutathione peroxidase (*GPX*), and glutathione *S*-transferase A1 (*GSTA1*) (data not shown). Submicromolar concentrations of arsenite were found to elicit BACH1 nuclear export and partial loss of DNA binding; however, maximum BACH1 inactivation was observed at micromolar concentrations in concert with NFE2L2 activation. In contrast, hemin treatment induces HMOX1 expression without activating NFE2L2 or inducing other NFE2L2-regulated genes. Given that BACH1 is thought to dominantly repress gene expression through competition with NFE2L2, it was surprising that only HMOX1 was induced when BACH1 was inactivated. Examination of BACH1 interactions at ARE enhancers of TXNRD1 and NQO1 (data not shown) demonstrated no detectable BACH1 binding by ChIP assay. Simultaneously, BACH1 binding at the β-globin LCR3 site (TGCTGAGTCATGATGAGTCAT) showed a 6-fold decrease without concurrent changes in β-globin expression (data not shown). Therefore, to uncover genes that are regulated by BACH1 in a manner similar to HMOX1, BACH1 expression was knocked down, and global gene expression was measured by microarray analysis. Again, we were surprised to observe that the loss of BACH1 is associated only with a very prominent up-regulation of HMOX1 and a small up-regulation of a few additional genes having unknown biologic significance.

Heme is vital for life and is an essential prosthetic group for proteins responsible for oxidative respiration, biosynthetic reactions, and detoxification of xenobiotics (*e.g.* mitochondrial cytochromes, monooxygenases, dioxygenases, catalase, peroxidases, nitric oxide synthase, and guanylate cyclase). All cells possess an intracellular pool of free heme through which newly synthesized and recycled heme molecules pass on their way to being incorporated into newly synthesized hemoproteins. The intact heme molecule is a potentially cytotoxic iron chelate, attributable to its ability to catalyze peroxidation of membrane lipids and formation of reactive oxygen species (15). The ability of heme to catalyze reactive oxygen species formation dictates that cells strike a homeostatic balance between maintaining an adequate heme supply for hemoprotein synthesis and the lowest possible concentration to minimize redox damage. Thus, inducible HMOX1 fulfills a vital role in preventing toxicity associated with excessive heme accumulation. Furthermore, in contrast to heme itself, the products released by HMOX activity have anti-oxidant properties (15, 46). Opening of the porphyrin ring releases CO, biliverdin, and iron. Bilirubin, the reduced product of biliverdin, has anti-oxidant properties (15, 46), whereas iron rapidly induces ferritin synthesis (47), which sequesters and oxidizes free iron. Thus, in addition to lowering levels of pro-oxidant heme molecule, increased HMOX1 activity results in the formation of reaction end products that have

antioxidant activities that provide a measure of protection against intracellular oxidative stress.

In this model, BACH1 serves as a fulcrum balancing the physiologic need for free heme with efficient heme metabolism. Elevated levels of intracellular heme inactivate BACH1 leading to loss of HMOX1 repression (35, 48). Thus, BACH1 is well situated as a central regulator of cellular heme homeostasis by reciprocally repressing degradation when intracellular heme concentrations are low and inducing HMOX1-mediated degradation when heme concentrations are high. This sensitivity of BACH1 to heme implies that BACH1 acts as a rheostat regulating intracellular free heme levels. Furthermore, because BACH1 is a cysteine-rich protein sensitive to redox regulation (35), it functions as a sensor of oxidative stress that protects cells by limiting heme-catalyzed reactive oxygen species production through catalysis of intracellular heme and increasing formation of HMOX1 reaction products that possess antioxidant properties. Thus, the sensitivity of BACH1 to intracellular redox status allows BACH1 to act as a protective fail-safe mechanism against the free radical formation catalyzed by free heme.

Acknowledgment—We thank Dr. N. Fusenig (Division of Differentiation and Carcinogenesis in Vitro, German Cancer Research Center, Heidelberg, Germany) for the gift of HaCaT keratinocytes.

REFERENCES

1. Yoshida, T., and Kikuchi, G. (1978) *J. Biol. Chem.* **253,** 4230–4236
2. Hayashi, S., Omata, Y., Sakamoto, H., Higashimoto, Y., Hara, T., Sagara, Y., and Noguchi, M. (2004) *Gene* (*Amst.*) **336,** 241–250
3. Sardana, M. K., Sassa, S., and Kappas, A. (1982) *J. Biol. Chem.* **257,** 4806–4811
4. Sunderman, F. W., Jr. (1987) *Ann. N. Y. Acad. Sci.* **514,** 65–80
5. Tenhunen, R., Marver, H. S., and Schmid, R. (1970) *J. Lab. Clin. Med.* **75,** 410–421
6. Alam, J., Shibahara, S., and Smith, A. (1989) *J. Biol. Chem.* **264,** 6371–6375
7. Reichard, J. F., Motz, G. T., and Puga, A. (2007) *Nucleic Acids Res.* **35,** 7074–7086
8. Cho, H. Y., Jedlicka, A. E., Reddy, S. P., Kensler, T. W., Yamamoto, M., Zhang, L. Y., and Kleeberger, S. R. (2002) *Am. J. Respir. Cell Mol. Biol.* **26,** 175–182
9. Gong, P., Hu, B., Stewart, D., Ellerbe, M., Figueroa, Y. G., Blank, V., Beckman, B. S., and Alam, J. (2001) *J. Biol. Chem.* **276,** 27018–27025
10. Okinaga, S., and Shibahara, S. (1993) *Eur. J. Biochem.* **212,** 167–175
11. Shibahara, S., Muller, R. M., and Taguchi, H. (1987) *J. Biol. Chem.* **262,** 12889–12892
12. Lee, P. J., Jiang, B. H., Chin, B. Y., Iyer, N. V., Alam, J., Semenza, G. L., and Choi, A. M. (1997) *J. Biol. Chem.* **272,** 5375–5381
13. Vile, G. F., Basu-Modak, S., Waltner, C., and Tyrrell, R. M. (1994) *Proc. Natl. Acad. Sci. U. S. A.* **91,** 2607–2610
14. Vile, G. F., and Tyrrell, R. M. (1993) *J. Biol. Chem.* **268,** 14678–14681
15. Ryter, S. W., and Tyrrell, R. M. (2000) *Free Radic. Biol. Med.* **28,** 289–309
16. Spuches, A. M., Kruszyna, H. G., Rich, A. M., and Wilcox, D. E. (2005) *Inorg. Chem.* **44,** 2964–2972
17. Kann, S., Estes, C., Reichard, J. F., Huang, M. Y., Sartor, M. A., Schwemberger, S., Chen, Y., Dalton, T. P., Shertzer, H. G., Xia, Y., and Puga, A. (2005) *Toxicol. Sci.* **87,** 365–384
18. Furukawa, M., and Xiong, Y. (2005) *Mol. Cell Biol.* **25,** 162–171
19. McMahon, M., Itoh, K., Yamamoto, M., and Hayes, J. D. (2003) *J. Biol. Chem.* **278,** 21592–21600
20. Zhang, D. D., and Hannink, M. (2003) *Mol. Cell Biol.* **23,** 8137–8151
21. Amoutzias, G., Veron, A., Weiner, A., Robinson-Rechavi, M., Bornberg-Bauer, E., Oliver, S., and Robertson, D. (2006) *Mol. Biol. Evol.* **24,** 827–835
22. Itoh, K., Chiba, T., Takahashi, S., Ishii, T., Igarashi, K., Katoh, Y., Oyake, T., Hayashi, N., Satoh, K., Hatayama, I., Yamamoto, M., and Nabeshima, Y. (1997) *Biochem. Biophys. Res. Commun.* **236,** 313–322
23. Wasserman, W. W., and Fahl, W. E. (1997) *Proc. Natl. Acad. Sci. U. S. A.* **94,** 5361–5366
24. Motohashi, H., O'Connor, T., Katsuoka, F., Engel, J. D., and Yamamoto, M. (2002) *Gene* **294,** 1–12
25. Wang, X., Tomso, D. J., Chorley, B. N., Cho, H. Y., Cheung, V. G., Kleeberger, S. R., and Bell, D. A. (2007) *Hum. Mol. Genet.* **16,** 1188–1200
26. Venugopal, R., and Jaiswal, A. K. (1996) *Proc. Natl. Acad. Sci. U. S. A.* **93,** 14960–14965
27. Kanezaki, R., Toki, T., Yokoyama, M., Yomogida, K., Sugiyama, K., Yamamoto, M., Igarashi, K., and Ito, E. (2001) *J. Biol. Chem.* **276,** 7278–7284
28. Igarashi, K., Hoshino, H., Muto, A., Suwabe, N., Nishikawa, S., Nakauchi, H., and Yamamoto, M. (1998) *J. Biol. Chem.* **273,** 11783–11790
29. Oyake, T., Itoh, K., Motohashi, H., Hayashi, N., Hoshino, H., Nishizawa, M., Yamamoto, M., and Igarashi, K. (1996) *Mol. Cell Biol.* **16,** 6083–6095
30. Sun, J., Hoshino, H., Takaku, K., Nakajima, O., Muto, A., Suzuki, H., Tashiro, S., Takahashi, S., Shibahara, S., Alam, J., Taketo, M. M., Yamamoto, M., and Igarashi, K. (2002) *EMBO J.* **21,** 5216–5224
31. Sun, J., Brand, M., Zenke, Y., Tashiro, S., Groudine, M., and Igarashi, K. (2004) *Proc. Natl. Acad. Sci. U. S. A.* **101,** 1461–1466
32. Igarashi, K., and Sun, J. (2006) *Antioxid. Redox. Signal.* **8,** 107–118
33. Brand, M., Ranish, J. A., Kummer, N. T., Hamilton, J., Igarashi, K., Francastel, C., Chi, T. H., Crabtree, G. R., Aebersold, R., and Groudine, M. (2004) *Nat. Struct. Mol. Biol.* **11,** 73–80
34. Shan, Y., Lambrecht, R. W., Ghaziani, T., Donohue, S. E., and Bonkovsky, H. L. (2004) *J. Biol. Chem.* **279,** 51769–51774
35. Ishikawa, M., Numazawa, S., and Yoshida, T. (2005) *Free Radic. Biol. Med.* **38,** 1344–1352
36. Dohi, Y., Alam, J., Yoshizumi, M., Sun, J., and Igarashi, K. (2006) *Antioxid. Redox. Signal.* **8,** 60–67
37. Ohira, M., Seki, N., Nagase, T., Ishikawa, K., Nomura, N., and Ohara, O. (1998) *Genomics* **47,** 300–306
38. Ogawa, K., Sun, J., Taketani, S., Nakajima, O., Nishitani, C., Sassa, S., Hayashi, N., Yamamoto, M., Shibahara, S., Fujita, H., and Igarashi, K. (2001) *EMBO J.* **20,** 2835–2843
39. Tahara, T., Sun, J., Nakanishi, K., Yamamoto, M., Mori, H., Saito, T., Fujita, H., Igarashi, K., and Taketani, S. (2004) *J. Biol. Chem.* **279,** 5480–5487
40. Boukamp, P., Petrussevska, R. T., Breitkreutz, D., Hornung, J., Markham, A., and Fusenig, N. E. (1988) *J. Cell Biol.* **106,** 761–771
41. Sartor, M., Schwanekamp, J., Halbleib, D., Mohamed, I., Karyala, S., Medvedovic, M., and Tomlinson, C. R. (2004) *BioTechniques* **36,** 790–796
42. Guo, J., Sartor, M., Karyala, S., Medvedovic, M., Kann, S., Puga, A., Ryan, P., and Tomlinson, C. R. (2004) *Toxicol. Appl. Pharmacol.* **194,** 79–89
43. Smyth, G. K. (2004) *Stat. Appl. Genet. Mol. Biol.* **3,** Article3
44. Dudoit, S., Yang, Y. H., Callow, M. J., and Speed, T. P. (2002) *Statistica Sinica* **12,** 111–139
45. Sartor, M. A., Tomlinson, C. R., Wesselkamper, S. C., Sivaganesan, S., Leikauf, G. D., and Medvedovic, M. (2006) *BMC. Bioinformatics* 7:538
46. Stocker, R., Yamamoto, Y., McDonagh, A. F., Glazer, A. N., and Ames, B. N. (1987) *Science* **235,** 1043–1046
47. Eisenstein, R. S., and Munro, H. N. (1990) *Enzyme* **44,** 42–58
48. Suzuki, H., Tashiro, S., Hira, S., Sun, J., Yamazaki, C., Zenke, Y., Ikeda-Saito, M., Yoshida, M., and Igarashi, K. (2004) *EMBO J.* **23,** 2544–2553